Contribution to Characterisation of Insect-Proof Screens: Experimental Measurements in Wind Tunnel and CFD Simulation

D.L. Valera, F.D. Molina, A.J. Álvarez and J.A. López
Dept. of Rural Engineering, Univ. of Almería, Ctra. Sacramento, 04120 Almería
Spain

J.M. Terrés-Nicoli and A. Madueño
CEAMA, Univ. of Granada, Avda. del Mediterráneo s/n, 18071 Granada
Spain

Keywords*:* porous media, airflow, pressure drop, permeability, ventilation

Abstract

The aim of the present study was to evaluate geometrical characteristics and airflow resistance of eleven different insect-proof screens by three different experimental procedures: equipment based in water-flow suction, low-speed wind tunnel, and CFD simulations. The two first arrangements had the same principle, in that air was forced through the test samples in order to create a pressure drop. Last analyses were carried out by numerical simulations of airflow through insect-proof screens using a commercial fluid dynamics code based in Finite Element method (ANSYS/ FLOTRAN v8.0). Previously, an analysis images system, called EUCLIDES v1.1, was designed with MS Visual Basic 6.0 running under MS Windows, for the analysis of the screens samples images captured with a microscope. A geometrical characterization of the eleven screens materials was carried out using this software tool. The software allows to determine all the geometric parameters that characterize the screens, as thread diameter and distances between two adjacent threads in two directions, from the four coordinates that defined each pore. The results obtained in this work show that the eleven screens can be classed in three groups, corresponding with the fibre density, with similar porosity and airflow properties (permeability and inertial factor). However, sample 8 has a small thread diameter and screen thickness that decreased the pressure drop coefficient. The results suggest that equations based on the porosity of the screen and the Reynolds number can be used to calculate the pressure drop coefficient.

INTRODUCTION

In an integrated pest management system, exclusion of pests should be one of the first tactics considered to reduce the need for other control measures. Whiteflies (*Bemisia tabaci*) and thrips (*Frankliniella occidentalis*) are among the most important pests of greenhouse crops in Almería (Acebedo, 2004). As in other parts of the world (Taylor et al., 2001), most of the losses produced in Spain by *Bemisia tabaci* are due to its role as a virus vector (Guirao et al., 1997). Tomato yellow leaf curl virus (TYLCV) was reported for the first time in Spain in the autumn of 1992 (Moriones et al., 1993).

Because of pest-acquired resistance, management practices that rely on insecticides are growing increasingly less effective, and less environmentally and economically appropriate. Reductions in pest populations (Baker and Jones, 1989) and lower incidence of insect-transmitted diseases (Baker and Jones 1989, 1990) have been documented when screening is used. Exclusion screens for the greenhouse may become a necessary alternative to pesticide use.

However, airflow resistance, primarily a function of hole or mesh size, reduces the ventilation rate. Many efficacious screens have a small hole size and are more resistant to airflow than are more open-meshed screens (Bethke and Paine, 1991; Bell and Baker, 2000). The aim of the present study was to evaluate geometrical characteristics and airflow resistance of eleven different insect-proof screens by three different experimental procedures: low-speed wind tunnel, equipment based in water-flow suction, and CFD simulations.

Proc. IC on Greensys
Eds.: G. van Straten et al.
Acta Hort. 691, ISHS 2005

MATERIALS AND METHODS

In order to obtain the airflow characteristics of porous screens we measured the pressure drop caused by the insect-proof screen for different velocities in the range 0.1 to 12 m s^{-1}. The first experiments were carried out in a wind tunnel with a cross-section of 420 mm × 360 mm and 5.2 m long. A helicoidally fan of 460 mm diameter driven by multi-speed 2.2 kW 3-phase induction electric motor HCT-45 (Sodeca S.A., Sant Qurze de Besora, Spain). Airflow was controlled by a Micromaster 420 AC inverter (Siemens Energy & Automation Inc., Alpharetta, USA) that allow decreased the fan motor speed from 0 to 2865 rpm, with digital microprocessor control and a set point resolution of 0.01 Hz. The static pressure drop through the screen was measured by a pressure transducer SETRA (Setra Systems Inc., Boxboruogh, USA), connected to two Pitot tubes, one 430 mm upstream and one 430 mm downstream from the tested screens (Terrés-Nicoli et al., 2004.). Air velocity was determined connecting the static pressure and total pressure tapings of the upstream Pitot tube to another pressure transducer MKS (MKS Instrument Inc., Andover, USA).

For air velocity lower to 1 m s^{-1} the screen samples (diameter 115 mm) were mounted in a test duct (length 220 mm) separated by PVC rings of 10 mm thickness, 70 mm internal and 115 mm external diameter containing 20 screen samples (Fig. 1). Originally, the downstream tube was connected to the upper side of a water reservoir by a flexible pipe. The measurements are based on the pressure drop caused by natural suction of air through the samples as a result of water flow induced by gravity (Miguel et al., 1997). Subsequently, we repeated the test for the sample number 1, for air velocity between 0.1 and 1 m s^{-1}, connecting the downstream tube to a fan NMB-4715KL (NMB Technologies Inc, Chatsworth, USA). The airflow supplied by the fan was regulated by controlling the rotational speed of the fan, function of the voltage that was varied from 3 V to 12 V with a DC power supply HY-3010 (DavJones Technology, Singapore). No statistical differences were observed between the tests made with the fan and the water reservoir for sample number 1. For reason of simplicity, we use the fan for air supply with the rest of samples (from 2 to 11). The pressure drop was measured using an inclined tube manometer AIRFLOW type 504 (Airflow Developments Limited, Buckinghamshire, England). The manometer, with a full-scale range of 125 Pa and an accuracy of 1 Pa, was connected to two Pitot tubes (150 mm upstream and 90 mm downstream). The measurement of air velocity was taken using a multifunction digital handheld instrument TESTO® 445 (Testo S.A., Cabrils, Spain) with a hot-bulb probe. This instrument has a measurement range from 0 to 10 m s^{-1} with an accuracy of ±0.03 m s^{-1} and resolution of 0.01 m s^{-1}. The equipment also contains a temperature probe (thermistor NTC) with a range of –20 to 70ºC and an accuracy of ±0.4ºC.

Last analyses were carried out by numerical simulations of airflow through insect-proof screens using a commercial fluid dynamics code based in Finite Element Method (ANSYS/FLOTRAN v8). In the simulation, it was assumed that a woven screen comprises a large number of small pores, and a similar flow passed through each. The pore was modelled as the intersection of four cylinder (Teitel and Shklyar, 1998). Previously, an analysis images system, named EUCLIDES v1.1, was designed with MS Visual Basic 6.0 running under MS Windows, for the analysis of the screens samples images captured with a microscope DMWB1 (Motic Spain S.L., Barcelona, Spain). We used a plan 4X achromatic lens that provided images with a resolution of 0.0105 mm/pixel. Once the image was captured a different program (Photo Finish 4.0) was used to convert the images in true colour to black and white. A geometrical characterization of the eleven screens materials was carried out using the EUCLIDES software. This software allows to determine all the geometric parameters that characterize the screens, as thread diameter, d, and distances between two adjacent threads in two directions, D_{hx} and D_{hy}, from the four coordinates that defined each pore, recognised automatically by the software. The program also measures the porosity as the ratio of geometric pore area, calculated from the vertices coordinates, to whole area. For all screens we analysed three samples of 1 cm^2 size.

RESULTS

Airflow Characteristics of Insect-proof Screens

Darcy's equation is linear in velocity, u, for Reynolds number ($Re_p=\rho u K_p^{1/2}/\mu$) lower than unity. However, for $Re_p>10$ a breakdown in linearity have observed, due to the fact that the form drag due to solid obstacles (screen) is comparable with surface drag due to friction (Nield and Bejan, 1998). The flow of air through a porous mesh (very porous medium) can be described by a modification of the Darcy's equation (Forchheimer, 1901):

$$\frac{\partial P}{\partial x} = -\left(\frac{\mu}{K_p} \cdot u + \rho \cdot \left(\frac{Y}{K_p^{1/2}} \right) \cdot |u| \cdot u \right) \tag{1}$$

where K_p is a coefficient independent of the nature of the fluid but it depends on the geometry of the medium. It has dimensions $(\text{length})^2$ and is called the specific permeability of the medium (Nield and Bejan, 1998). Y is a dimensionless form-drag constant dependent of the nature of the porous medium, called inertial factor. Air dynamic viscosity, μ, air density, ρ, are known (from measured temperature for each test).

According to the Forchheimer's equation, a second-order polynomial has been used for fitting the experimental values of pressure drop through a screen (Miguel et al., 1997; Muñoz et al., 1999; Dierickx, 1998):

$$\Delta P = au^2 + bu + c \tag{2}$$

For each material tested, the data resulting from the experiments performed were plotted as pressure drop versus the velocity as show Fig. 2. In all the samples tested, the equation that best seemed to fit the curves obtained was the second order polynomial, Eq. (2). The coefficients are presented in Table 1. Therefore, provided the best-fit coefficients, zero order term can be neglected compared with the other terms. Equating the first- and second-order terms, respectively, of the experimental polynomial and the Forchheimer's equation (1), the permeability and the inertial factor can be obtained:

$$K_p = \Delta x \frac{\mu}{b} \qquad\qquad Y = \frac{a K_p^{0.5}}{\Delta x \rho} \tag{3}$$

where screen thickness, Δx, was measured from image analysis (EUCLIDES v1.1). We have calculated the permeability K_p and inertial factor Y from equation (3). The results are listed in Table 2.

Pressure Drop Coefficient for Screens

Bernoulli's equation can be also used to describe the relationship between pressure drop and air velocity through the screens (Kosmos et al., 1993; Montero et al., 1997; Teitel and Shklyar, 1998):

$$\Delta P = \tfrac{1}{2} F_s \rho u^2 \tag{4}$$

where F_s is the pressure drop coefficient. This coefficient can be used to predict the pressure drop through screens even at $Re_p<150$ (Teitel, 2001). Brundrett (1993) suggests an expression for the pressure loss coefficient:

$$F_s = \left[\frac{\sigma_m}{\sigma_k} \frac{7.125}{\text{Re}} + \frac{0.88}{\log(\text{Re}+1.25)} + 0.055 \log(\text{Re}) \right] \left[\frac{1-\alpha^2}{\alpha^2} \right] \tag{5}$$

where σ_k and σ_m are the kinetic energy and momentum correction factors, respectively. Bailey et al., (2003) used this equation as the basis for correlating the loss coefficients of five insect screen, resulting:

$$F_s = \left[\frac{18}{\mathrm{Re}} + \frac{0.75}{\log(\mathrm{Re}+1.25)} + 0.055\log(\mathrm{Re})\right]\left[\frac{1-\alpha^2}{\alpha^2}\right] \quad (6)$$

Ishizuka et al., 2000 studied the relationship between flow resistance coefficient F_s of wire nets and a group of two parameters, Reynolds number *Re* (based on the fibre diameter) and porosity coefficient, α (Pinker and Herbert, 1967). They obtained the following empirical correlation, applicable in the range of 0.4<*Re*<95, on the basis of the best fit to the measured data:

$$F_s = 28\left(\frac{\mathrm{Re}\,\alpha^2}{1-\alpha}\right)^{-0.95} \quad (7)$$

Linker et al. (2002) also calculated a loss coefficient as the product of a function of porosity and a function of the Reynolds number:

$$F_s = \left(\frac{13.0}{\mathrm{Re}} + 0.82\right)\left(\frac{1-\alpha^2}{\alpha^2}\right) \quad (8)$$

We have calculated the pressure drop coefficient substituting Eqs. (2) and (3) in Eq. (4) yields:

$$F_s = \frac{2\Delta x}{K_p^{0.5}}\left(\frac{1}{\mathrm{Re}_p} + Y\right) \quad (9)$$

The pressure drop coefficients obtained from Eq. (9) for all of samples tested are listed in Table 2. and compared with values calculated from the others equations (6,7,8) in Fig. 3.

DISCUSSION

Pressure drop for insect-proof screen used in greenhouse vents has been determined with both airflow suction (water flow suction for screen 1) and wind tunnel. Both methods give similar results in the air velocity common range of 0.5 to 1 m s^{-1}. The equations that better relates the screen permeability and inertial factor with porosity, are $K_p = 5.68 \times 10^{-8}\ \alpha^{3.68}$ and $Y = 0.0567\ \alpha^{-1.1604}$, respectively.

The results obtained in this work show that the eleven screens can be classed in three groups, corresponding with the fibre density, with similar porosity and airflow properties (permeability and inertial factor). However, sample 8 has small thread diameter and screen thickness that decreased the pressure drop coefficient. The results suggest that equations based on the porosity of the screen and the Reynolds number can be used for calculate the pressure drop coefficient.

Configuration with two cylinders in a plane (horizontal fibres) and the other two orthogonal to them (vertical fibres) in two parallel planes behind the horizontal fibres and in front of them, produced better results in CFD simulations.

ACKNOWLEDGEMENTS

This research was partially supported by the Projects C03-159 and CR-UAL-0202.

Literature Cited

Acebedo, M.M. 2004. *Bemisisa tabaci*, una de las principales plagas en cultivos bajo abrigo. Vida Rural, 189: 31-34. (In Spanish)

Bailey, B.J., Montero, J.I., Pérez Parra, J., Robertson, A.P., Baeza, E and Kamaruddin, R. 2003. Airflow resistance of greenhouse ventilators with and without insect screens. Biosystem Engineering, 86 (2): 217-229.

Baker, J.R. and Jones, R.K. 1989. Screening as part of insect and disease management in the greenhouse. N.C. Flower Growers' Bull., 34: 1–9.

Baker, J.R. and Jones, R.K. 1990. An update on screening as part of insect and disease management in the greenhouse. N.C. Flower Growers' Bull., 35: 1–3.

Bell, M.L. and Baker, J.R. 2000. Comparison of greenhouse screening materials for excluding whitefly (Homoptera: Aleyrodidae) and thrips (Thysanoptera: Thripidae). J. Econ. Entomol., 93 (3): 800-804.

Bethke, J.A. and Paine, T.D. 1991. Screen hole size and barriers for exclusion of insect pests of glasshouse crops. J. Entomol. Sci., 26: 169–177.

Dierickx, W. 1998. Flow reduction of synthetic screens obtained with both a water and airflow apparatus. J. Agric. Engng Res., 71: 67-73.

Forchheimer, P. 1901. Wasserbewegung durch Boden. Z. Vereines Deutscher Ingenieure, 45: 1782-1788.

Guirao, P., Beitia, F. and Cenis, J.L. 1997. Biotype determination of Spanish populations of *Bemisia tabaci* (Hemiptera: Aleyrodidae). Bulletin of Entomological Research , 87: 587–593.

Ishizuka, M., Hayama, S. and Peng, G. 2000. Measurement of flow resistance coefficients for wire nets in natural air convection flow. Proc. Sixth Triennal International Symposium on Fluid Control, Measurement and Visualization (FLUCOME 2000), Sherbrooke, Canada, 13-17 August, 6 pp.

Kosmos, S.R., Riskowski, G.L. and Christianson, L.L. 1993. Force and static pressure resulting from airflow through screens. Transactions of ASAE, 36 (5): 1467–1472.

Linker, R., Tarnopolsky, M. and Seginer, I. 2002. Increased resistance to flow and temperature-rise resulting from dust accumulation on greenhouse insect-proof screens. 2002 ASAE Annual International Meeting. Chicago, USA 28-31 July. 9 pp.

Miguel, A.F., Van de Braak, N.J. and Bot, G.P.A. 1997. Analysis of the airflow characteristics of greenhouse screening materials. J. Agric. Engng Res., 67: 105-112.

Montero, J.I., Muñoz, P. and Anton, A. 1996. Discharge coefficients of greenhouse windows with insect-proof screens. Acta Hortic., 443: 71-77.

Moriones, E., Arnó, J., Accotto, G.P., Noris, E. and Cavallarin, L. 1993. First report of tomato yellow leaf curl virus in Spain. Plant Disease, 77: 953.

Muñoz, P., Montero, J.I., Antón, A. and Giuffrida, F. 1999. Effect of insect-proof screens and roof openings on greenhouse ventilation. J. Agric. Engng Res., 73: 171-178.

Nield, D.A. and Bejan, A. 1999. Convection in porous media. Springer, New York (USA), 546 pp.

Pinker, R.A. and Herbert, M.V. 1967. Pressure loss associated with compressible flow through square-mesh wire gauzes. J. Mech. Engng. Sci., 9 (1): 11-23.

Taylor, R.A.J., Shalhevet, S., Spharim, I., Berlinger, M.I. and Lebiush-Mordechi S. 2001.- Economic evaluation of insect-proof screens for preventing tomato yellow curl virus tomatoes in Israel. Crop Protection, 20: 561-569.

Teitel, M. and Shklyar, A. 1998. Pressure drop across insect-proof screens. Trans. ASAE, 41(6): 1829-1834.

Teitel, M. 2001. The effect of insect-proof screens in roof openings on greenhouse micro-climate. Agric. and Forest Meteorology, 110: 13-25.

Terrés-Nicoli, J.M., Losada, M.A. and Cuesta Cañas, J.A. 2004. Estudio de Ingeniería de Viento de "Mallas de aireación de Invernaderos Tipo Almería". INV01-A03. CEAMA, Granada, Spain, 23 pp. (In Spanish).

Tables

Table 1. Geometrical properties of eleven insect-proof screens tested (porosity, α, thread diameter, D_f, screen hole size, $D_{hx} \times D_{hy}$, diameter inscribed circle, D_i, hole area, S_h) analysed with EUCLIDES.

N	*Trade name*	*Density* (fibre cm^{-2})	α (m^2 m^{-2})	D_{hx}(μm)	D_{hy} (μm)	D_f (μm)	D_i (μm)	S_h (mm^2)
2	Supertex-26 16x10	10.0×14.6	0.458	748,8±23.6	415.6±25.9	260.7	419.1±25.7	0.311
7	Sunsaver 16x10B	9.3×16.3	0.477	771.5±78.8	379.1±56.4	244.7	378.5±34.7	0.290
10	Econet F 16x10	9.5×15.4	0.483	789.7±87.2	410.0±63.0	253.5	407.6±54.3	0.322
1	Sunsaver 20x10W	18.6×9.4	0.371	267.8±35.6	795.3±28.9	271.0	272.9±35.2	0.213
3	Supertex-30 20x10	19.4×9.2	0.387	256.6±23.3	840.0±20.4	251.2	261.5±23.5	0.215
5	Bionet 20x10	19.6×9.5	0.367	245.5±21.1	804.9±20.1	258.4	251.7±21.0	0.198
9	Sunsaver 20x10	20.1×9.7	0.375	247.3±38.1	777.4±40.2	253.2	251.9±37.7	0.192
11	Econet SF 20x10	9.7×19.6	0.389	775.0±81.5	263.7±60.9	252.6	265.4±52.8	0.202
4	Sunsaver 23x11	22.2×10.4	0.319	194.9±17.6	711.7±29.7	251.8	199.7±17.8	0.139
6	Sunsaver 18x33	33.2×17.8	0.288	127.2±19.7	386.2±11.1	175.3	130.3±19.6	0.049
8	Econet T 30x20	30.7×19.8	0.336	162.6±21.8	334.6±33.9	165.45	165.6±20.5	0.054

Table 2. Permeability K_p, inertial factor Y and pressure drop coefficient, F_s, thickness screen Δx, and coefficients a and b of the equation $\Delta p = au^2 + bu + c$ for eleven insect-proof screens tested and their correlation coefficient R^2.

Code	K_p (m^2)	Y	F_s	Δx (μm)	a	b	c	R^2	*ND*
1	$1.91 \cdot 10^{-09}$	0.166	$20.05 \cdot (0.17 + Re_p^{-1})$	438.6	1.9678	4.2246	-1.2894	0.9993	189
2	$2.65 \cdot 10^{-09}$	0.151	$13.88 \cdot (0.15 + Re_p^{-1})$	357.5	1.2346	2.4831	-1.2382	0.9996	99
3	$1.97 \cdot 10^{-09}$	0.164	$18.18 \cdot (0.16 + Re_p^{-1})$	403.2	1.7570	3.7785	-1.2519	0.9997	99
4	$1.33 \cdot 10^{-09}$	0.186	$24.07 \cdot (0.19 + Re_p^{-1})$	438.2	2.6335	6.0971	-1.2691	0.9996	191
5	$2.17 \cdot 10^{-09}$	0.157	$19.73 \cdot (0.16 + Re_p^{-1})$	459.1	1.8272	3.9051	-1.2137	0.9998	99
6	$4.50 \cdot 10^{-10}$	0.266	$26.80 \cdot (0.27 + Re_p^{-1})$	284.3	4.2108	11.626	-2.3669	0.9989	191
7	$2.99 \cdot 10^{-09}$	0.143	$16.25 \cdot (0.14 + Re_p^{-1})$	444.0	1.3682	2.7394	-1.5589	0.9994	99
8	$4.57 \cdot 10^{-10}$	0.273	$26.30 \cdot (0.27 + Re_p^{-1})$	281.2	4.2549	11.301	-2.1815	0.9989	108
9	$1.88 \cdot 10^{-09}$	0.163	$17.55 \cdot (0.16 + Re_p^{-1})$	379.9	1.6884	3.7314	-0.9362	0.9995	191
10	$4.15 \cdot 10^{-09}$	0.136	$14.08 \cdot (0.14 + Re_p^{-1})$	453.6	1.1336	2.0136	-2.2909	0.9980	99
11	$1.70 \cdot 10^{-09}$	0.155	$17.03 \cdot (0.16 + Re_p^{-1})$	350.9	1.5655	3.7992	-0.8853	0.9990	191

Figures

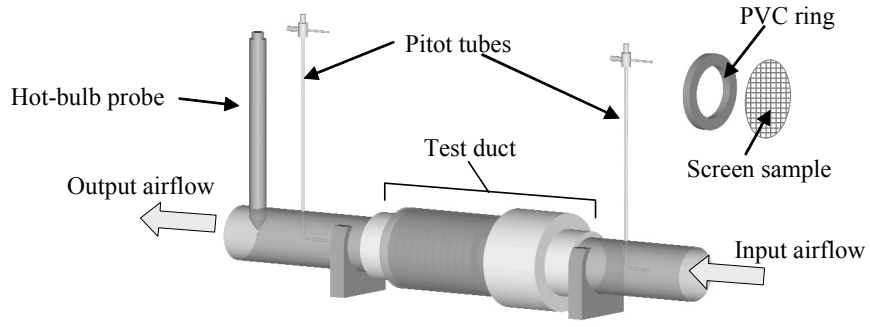

Fig. 1. Diagram of the apparatus for testing screens with Reynolds number less than 1.

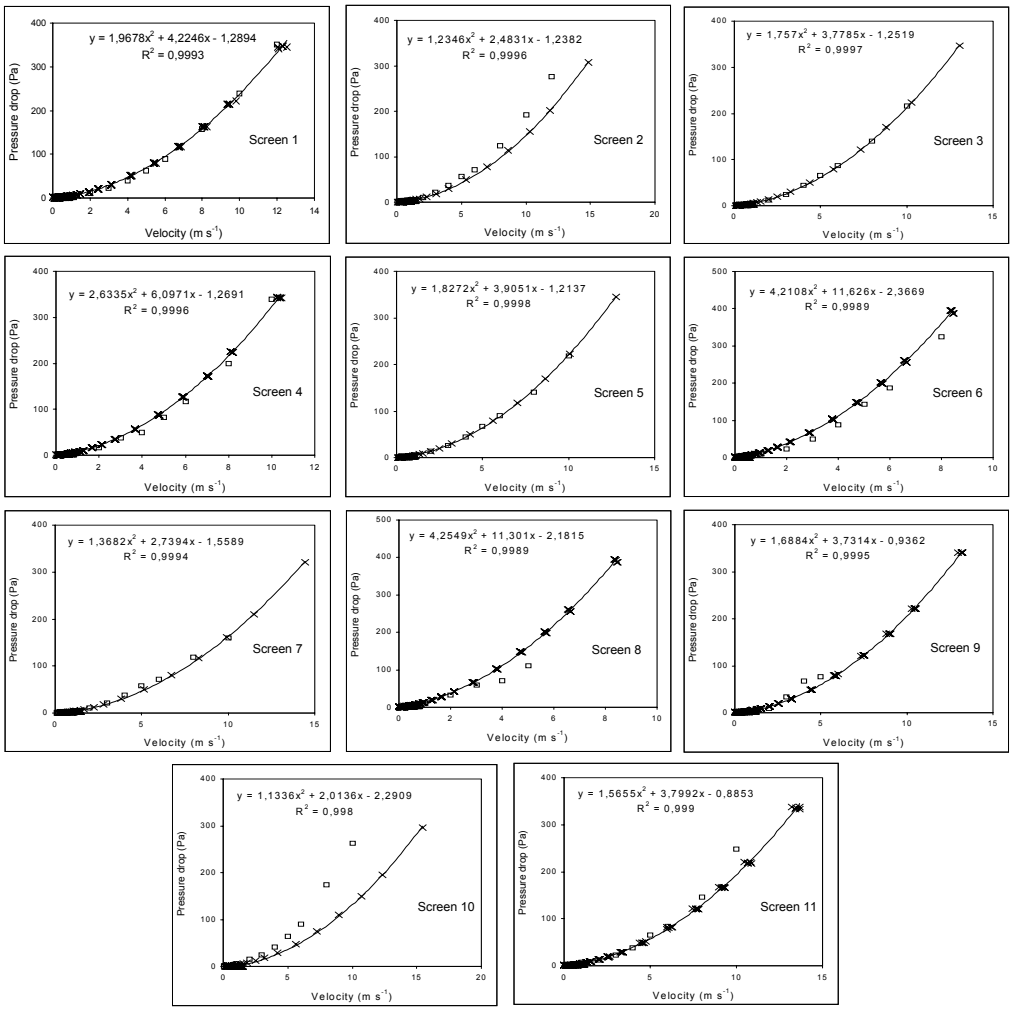

Fig. 2. Pressure drop for screens tested. Data from: (x) low-speed wind tunnel experiments and equipment based in water-flow suction, (□) CFD simulations and second order polynomial adjustment (line).

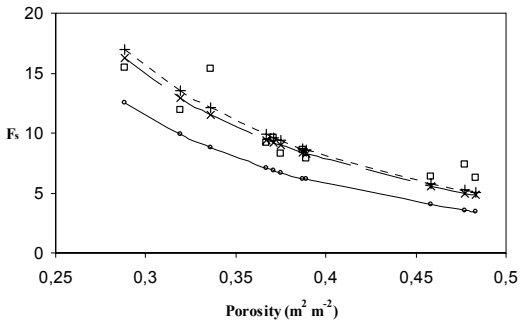

Fig. 3. Pressure drop coefficients of screens given by equations 6 (+), 7 (o) and 8 (x) and values derived from Eq. (9) and data of Table 2 (□) for Re=20 (Re_p=Re $K_p^{½}$ d_f^{-1}).